

On the Feasibility of Spatial Multiplexing for Indoor 60 GHz Communication*

Eric Torkildson, Upamanyu Madhow, and Mark Rodwell

Department of Electrical and Computer Engineering
University of California, Santa Barbara
Santa Barbara, CA 93106
etorkild@ece.ucsb.edu

ABSTRACT

We investigate spatial multiplexing in the sparse multipath environment characteristic of beamsteered indoor 60 GHz links. The small carrier wavelength implies that large spatial multiplexing gains are available even under line of sight (LOS) conditions for nodes with form factors compatible with consumer electronics devices such as set-top boxes and television sets. We present a transceiver architecture that provides both highly directive beams and spatial multiplexing, and model its performance for a typical in-room communication link. We evaluate the performance of a simple scheme using a fixed constellation, transmit beamsteering and MMSE reception. The performance is benchmarked against transmit precoding along the channel eigenmodes without a constellation constraint. We observe that, for a relatively small transmit power per antenna element (achievable, for example, in low-cost CMOS processes), the spatial multiplexing gain is robust to LOS blockage and to variations in the relative locations of the transmitter and receiver in the room.

Categories and Subject Descriptors

C.2.1 [Network Architecture and Design]: Wireless communication

General Terms

Design, performance, reliability

Keywords

60GHz, MIMO, capacity, mm-wave, mmWave, spatial multiplexing

*This research was supported in part by NSF grants CNS-0520335, ECS-0636621 and CNS-0832154.

Permission to make digital or hard copies of all or part of this work for personal or classroom use is granted without fee provided that copies are not made or distributed for profit or commercial advantage and that copies bear this notice and the full citation on the first page. To copy otherwise, to republish, to post on servers or to redistribute to lists, requires prior specific permission and/or a fee.

mmCom'10, September 24, 2010, Chicago, Illinois, USA.
Copyright 2010 ACM 978-1-4503-0142-8/10/09 ...\$10.00.

1. INTRODUCTION

There is significant interest in utilizing the 7 GHz of unlicensed spectrum at 60 GHz for indoor multiGigabit wireless networking, with applications such as high speed data sync, wireless high definition video, and Gigabit wireless local area networking. While the data rates offered by current and emerging mm-wave standards already exceed the rates achievable by lower-frequency links, speeds can be pushed further by applying multiple-input multiple-output (MIMO) processing techniques. To date, the spatial domain remains an untapped resource for increasing spectral efficiency at mm-wave frequencies. The small carrier wavelength at 60 GHz implies that spatial multiplexing gains are available even in LOS environments, as has been demonstrated in recent hardware prototypes [6]. In this paper, we investigate spatial multiplexing for a typical in-room communication link, with nodes having form factors consistent with consumer electronics devices such as set-top boxes and television sets (the form factor determines the available spatial multiplexing gain, as we observe later in this paper).

Our main results are as follows. We propose a transceiver architecture based on an array of subarrays, which provides both beamsteering gain (which reduces the power per antenna element and simplifies the receiver) and spatial multiplexing gain. We evaluate its performance in the sparse multipath environment resulting from highly directive transmissions using geometrical optics (i.e., ray tracing) to model the channel. We then consider a scheme with a constrained signal constellation, transmit beamsteering and MMSE reception, that more closely reflects practical hardware and signal processing limitations of current millimeter wave (mm-wave) systems. We conclude that the spatial multiplexing gain provided by our architecture is robust to LOS blockage and to variations in the locations of the transmitter and receiver within the room, while requiring a reasonably small power per transmit element realizable by low-cost CMOS processes.

The capacity of multi-antenna mm-wave links was previously studied in [1]. Although the propagation model used here is similar, we consider a system architecture that exploits an antenna spacing criterion shown to maximize the capacity of a LOS channel. Optimal antenna spacing was derived for linear arrays in [2] and [4]. In these works, the channel is modeled either as purely LOS or as a Rician channel, where a random non LOS (NLOS) component representing multipath is added to a deterministic LOS component to form the overall channel matrix. Here we adopt a de-

terministic ray-tracing model for both the LOS and NLOS components, which allows us to investigate how channel capacity is affected by node placement within a room. The validity of the ray-tracing approach has been supported by measurement studies at 60 GHz that observe sparse multipath environments [8].

2. MIMO ARCHITECTURE

Consider a MIMO link consisting of N_t transmit antennas and N_r receive antennas. Assuming frequency-flat fading, the received signal vector $\mathbf{r} \in \mathbb{C}^{N_r \times 1}$ is given by

$$\mathbf{r} = \mathbf{H}\mathbf{x} + \mathbf{w} \quad (1)$$

where $\mathbf{x} \in \mathbb{C}^{N_t \times 1}$ is the transmitted signal vector, $\mathbf{H} \in \mathbb{C}^{N_r \times N_t}$ is the channel matrix, $\mathbf{w} \in \mathbb{C}^{N_r \times 1}$ represents an additive white Gaussian noise vector with covariance $N_0\mathbf{I}_{N_r}$, and \mathbf{I}_N is the $N \times N$ identity matrix. The channel matrix \mathbf{H} can be decomposed as a sum of two components, with the first, \mathbf{H}_{LOS} , representing the LOS contribution, and the second representing the contribution of multipath. We now describe the LOS channel component in detail and review how the appropriate choice of antenna spacing results in a high-rank, orthonormal matrix. We then present a system architecture that exploits this result, and describe two alternative spatial processing schemes.

2.1 Antenna Spacing for LOS-MIMO

We first quickly review the concept of spatial multiplexing in LOS environments [4]. Consider two N -element ULAs aligned broadside and separated by distance R_o . The spacing between transmit antennas is given by d_T and the spacing between receive antennas is d_R . In the absence of multipath and additive noise, the received vector $\mathbf{r} \in \mathbb{C}^{N \times 1}$ is given by $\mathbf{r} = \mathbf{H}_{\text{LOS}}\mathbf{x}$, where $\mathbf{x} \in \mathbb{C}^{N \times 1}$ is the transmitted signal vector and $\mathbf{H}_{\text{LOS}} \in \mathbb{C}^{N \times N}$ is the LOS channel matrix. The (m, n) th entry of \mathbf{H}_{LOS} is given by

$$\begin{aligned} h(m, n) &= \frac{\lambda}{4\pi p(m, n)} e^{-j\frac{2\pi}{\lambda} p(m, n)} \\ &\approx \frac{\lambda}{4\pi R_o} e^{-j\frac{2\pi}{\lambda} \left(R_o + \frac{(md_R - nd_T)^2}{2R_o} \right)}, \end{aligned}$$

where the $p(m, n)$ is the distance between the n th transmit antenna and m th receive antenna, and the approximation $p(m, n) \approx R_o + \frac{(md_R - nd_T)^2}{2R_o}$ holds when the range is much greater than either array's length.

Let \mathbf{h}_k denote the receive array response to the k th transmit element (i.e., the k th column of \mathbf{H}_{LOS}). When the antenna spacing is small, $\mathbf{h}_k \approx \mathbf{h}_l$ for all $k, l = 1, 2, \dots, N$, and the channel matrix has rank one. By increasing the spacing by an appropriate amount, however, it is possible to produce a spatially uncorrelated channel matrix with full rank. Specifically, it can be shown that the inner product $(\mathbf{h}_k, \mathbf{h}_l) \approx 0$ for $k \neq l$ when the inter-element spacing satisfies the condition

$$d_T d_R = \frac{R_o \lambda}{N}. \quad (2)$$

When this condition is met, \mathbf{H}_{LOS} is a scaled unitary matrix with N equal singular values. This array geometry maximizes the Shannon capacity at moderate to high SNR, and we therefore refer to a pair of arrays satisfying (2) as optimal ULAs.

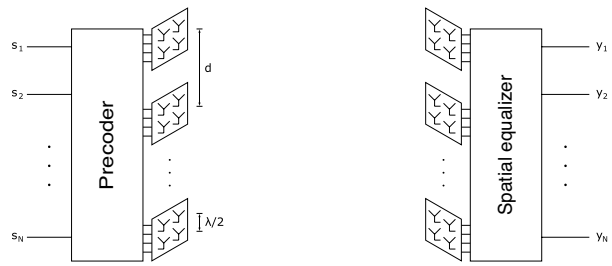


Figure 1: Proposed MIMO architecture. Each node possesses a linear array of N $\lambda/2$ -spaced uniform square subarrays.

2.2 Transceiver Architecture

Our proposed MIMO transceiver architecture in Fig. 1 is based on the preceding optimal spacing criterion. N independent data streams are precoded and transmitted over an N -element optimal ULA, where the spacing d is chosen to satisfy (2) given an expected link range R_o . Each element of the ULA is a square $\lambda/2$ -spaced subarray, which can be implemented as a monolithic millimeter-wave integrated circuit. Because the spacing between subarray elements is small, the subarrays provide array gain rather than spatial multiplexing gain. The additional directivity helps to offset propagation loss at mm-wave frequencies and attenuate multipath. Each subarray is an $M \times M$ square array, so the total number of antennas per node is given by $N_T = NM^2$. The receiver consists of an identical array-of-subarrays structure, with received signals feeding into an equalizer designed to null spatial interference. We assume herein that the architecture uses one of the following two transmission schemes.

Eigenmode Transmission: Our performance benchmark is standard waterfilling based eigenmode transmission. This employs a transmit precoder and a receive spatial equalizer based on the singular value decomposition (SVD) of the channel matrix \mathbf{H} , such that the channel is decomposed into N non-interfering parallel subchannels, or eigenmodes. The transmit powers along the eigenmodes are chosen, subject to a total power constraint, based on waterfilling. Given the space constraints, we do not provide a detailed description of this well-known scheme.

Transmit Beamsteering/Receive MMSE: While eigenmode transmission provides an upper bound on link performance, it is important to identify more conservative performance estimates that respect typical hardware and signal processing constraints. To this end, consider a scheme in which the transmitter sends a single data stream from each subarray, with each subarray limited to beamsteering in a given direction. We assume the transmitter knows the directions of the LOS and first-order reflection paths to the receiver (these can be learned by scanning at start-up), and beamsteering is constrained along these paths, with the array phases depending on the azimuthal and polar steering angles. The transmitter beamsteers in the direction(s) that maximize the sum-rate spectral efficiency. The constellation per data stream is fixed, and the transmit power is split evenly among the streams. The spatially multiplexed data streams can now interfere with each other, and we employ linear MMSE spatial interference suppression to separate them out at the receiver. The spectral efficiency is computed based on the SINR at the output of the MMSE

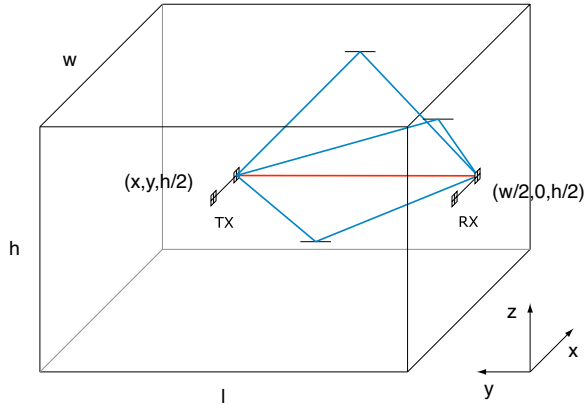


Figure 2: Indoor environment model showing LOS and first-order propagation paths.

equalizer, with the interference treated as Gaussian noise, and with the symbol constellation constrained to 16QAM. Details are omitted due to lack of space.

3. INDOOR ENVIRONMENT MODEL

The optimal antenna spacing criterion given by (2) assumes the transmit and receive arrays are aligned parallel, the channel is purely LOS, and the link range is known *a priori*. For practical indoor applications, none of these assumptions hold, and we wish to evaluate the performance of the proposed architecture when operating under more realistic scenarios. We therefore present an indoor environment propagation model that allows us to assess the impact of multipath propagation, link range variations, and LOS blockage. The propagation environment, shown in Fig. 2, is a room of dimensions $w \times l \times h$. The receiver's position is fixed at the center of the front wall at coordinates $(w/2, 0, h/2)$. The transmitter's position is variable, and given by coordinates $(x, y, h/2)$, where $0 \leq x \leq w$ and $0 \leq y \leq l$. The ULAs lie horizontally and the ULAs and their subarrays are parallel to the xz plane.

Given the specular nature of mm-wave reflections, we model the environment using the method of geometrical optics [7]. The LOS paths from transmitter to receiver, as well as single-bounce reflected paths off the side walls and ceiling, contribute to the channel matrix \mathbf{H} . Higher order reflections are disregarded in the simulations due to the additional path losses and reflection losses they incur, as well as the directivity provided by the subarrays. The channel matrix $\mathbf{H} \in \mathbb{C}^{N_T \times N_T}$ can be written

$$\mathbf{H} = \mathbf{H}_{\text{LOS}} + \mathbf{H}_{\text{L}} + \mathbf{H}_{\text{R}} + \mathbf{H}_{\text{C}}, \quad (3)$$

where \mathbf{H}_{LOS} is the LOS component, \mathbf{H}_{L} and \mathbf{H}_{R} are the components resulting from the left and right wall reflections, respectively, and \mathbf{H}_{C} is the contribution of the ceiling reflections. The (m, n) th entry of \mathbf{H}_{LOS} is given by

$$h_{\text{LOS}}(m, n) = \frac{\lambda}{4\pi p_{\text{LOS}}(m, n)} e^{-i \frac{2\pi}{\lambda} p_{\text{LOS}}(m, n)}. \quad (4)$$

The (m, n) th entry of \mathbf{H}_{L} is given by

$$h_{\text{L}}(m, n) = \Gamma(\theta_{\text{L}}) \frac{\lambda}{4\pi p_{\text{L}}(m, n)} e^{-i \frac{2\pi}{\lambda} p_{\text{L}}(m, n)}, \quad (5)$$

where $p_{\text{L}}(m, n)$ is the length of the path from the n th transmit antenna to the point of reflection on the left wall to the m th receive antenna, θ_{L} is the reflected ray's angle of incidence, and $\Gamma(\theta_{\text{L}})$ is the Fresnel reflection coefficient [3]. The entries of \mathbf{H}_{R} and \mathbf{H}_{C} are similarly defined, with appropriate substitutions of $p_{\text{R}}(m, n)$ or $p_{\text{C}}(m, n)$ for $p_{\text{L}}(m, n)$ and θ_{R} or θ_{C} for θ_{L} . Side wall reflections use the parallel reflection coefficient, while ceiling reflections use the perpendicular reflection coefficient. We assume the floor is carpeted, and we hence ignore floor reflections due to the high reflection loss of carpeted surfaces [5].

We model LOS blockage, referred to henceforth as the NLOS scenario, by removing the \mathbf{H}_{LOS} term from (3).

4. SIMULATION RESULTS

In this section, we evaluate the spectral efficiency achieved by the mm-wave MIMO architectures presented in Section 2 under the proposed indoor propagation model. The system and environment parameters are as follows. The room dimensions are $5 \text{ m} \times 5 \text{ m} \times 3 \text{ m}$. The spacing between subarrays, given by $d = \sqrt{2.5\lambda/N}$, is chosen such that the LOS component of the channel is spatially uncorrelated when the transmit node is located at the center of the room. The subarrays are 4×4 square subarrays. The overall array length is thus $L = (N - 1)d + 1.5\lambda$ (e.g., 8.7 cm for $N = 2$). The link operates at a carrier frequency of 60 GHz, with a corresponding wavelength of $\lambda = 5 \text{ mm}$. The noise power at the receiver is given by $P_N = kTBF$, where k is the Boltzmann constant, $B = 2.16 \text{ GHz}$ is the bandwidth, $T = 300 \text{ K}$ is the operating temperature, and $F = 10 \text{ dB}$ is the noise figure. The relative dielectric constant $\epsilon_r = 2.8$ and conductivity $\sigma = 0.221$ of the wall and ceiling surfaces are chosen to represent plasterboard [5].

4.1 Performance with Eigenmode Transmission

Fig. 3 plots the channel capacity of the eigenmode transmission scheme, averaged over random transmitter coordinates, as a function of P_A , the average transmit power per antenna, which is related to the total transmit power constraint by $P_T = NM^2 P_A$. (In practice, each antenna element would be peak power limited, which is a constraint we impose on the more practical beamsteering/MMSE scheme considered next.) For this plot, we consider the transmitter's x and y coordinates to be independent random variables uniformly distributed over $[0 + L/2, 5 - L/2]$. The number of data streams considered is $N = 1, 2, 3$, where $N = 1$ corresponds to transmitting a single data stream using a single subarray per node, with data transmitted along the dominant eigenmode. Increasing N to 2 or 3 results in roughly doubling or tripling the average channel capacity, respectively. The effect of increasing N is greater in NLOS settings, represented by dashed lines.

Fig. 4 depicts how the channel capacity varies as a function of the transmitter's position within the room. Here we have set $N = 2$ and fixed the transmit power per antenna at $P_A = -10 \text{ dBm}$. The shade of gray at a particular value of (x, y) indicates the channel capacity when the transmitter is located at coordinates (x, y) . The plot can be interpreted as a top-down view of the room with the receiver located at $(2.5, 0)$. The capacity is primarily affected by two factors. One is path loss, which causes the received signal power, and hence capacity, to decrease as the transmitter moves farther

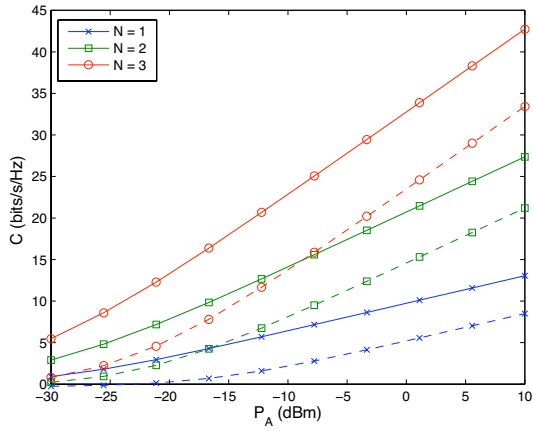


Figure 3: Channel capacity under eigenmode transmission scheme. Dashed lines represent the NLOS scenario.

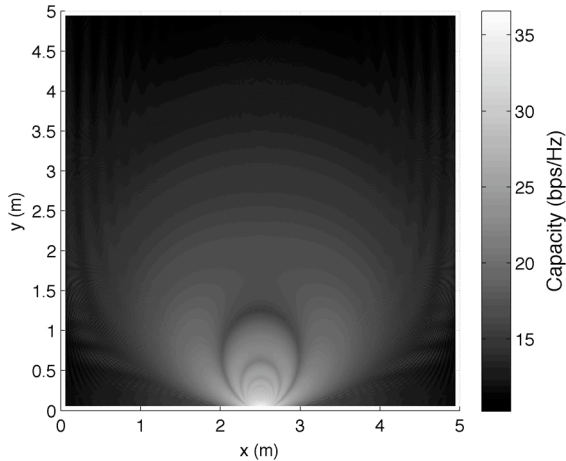


Figure 4: Channel capacity with eigenmode transmission as a function of transmitter coordinates.

from the receiver. The second is spatial correlation, which reduces spatial multiplexing gains. Given the proposed architecture, we have a 32×32 channel matrix. We expect two of the thirty-two eigenmodes to be dominant when the spatial correlation between subarrays is low. This happens, for instance, when the transmitter is placed at the center of the room and the optimal ULA criterion is satisfied. At other locations, however, when spatial correlation is high, the second eigenmode becomes much weaker than the first. As the transmitter moves from the center of the room towards the receiver, for instance, a series of rings alternating between low and high correlation is observed. These particular fluctuations arise from the correlation in the LOS component of the channel matrix and are independent of the multipath environment.

Fig. 5 plots the capacity as a function of the transmitter's position assuming LOS blockage. As expected, the absence of the dominant LOS signal component results in lower SNR and capacity throughout the room. In contrast to the LOS scenario, however, the NLOS channel does not become significantly ill-conditioned. We observe small-scale fluctuations in capacity that occur over very small distances. They

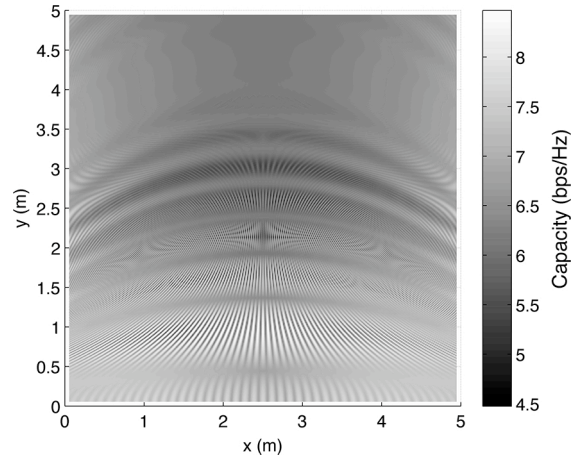


Figure 5: Channel capacity with eigenmode transmission scheme assuming LOS blockage.

fluctuations are as large as approximately 2 bps/Hz and can occur over distances on the order of millimeters. This suggests that, especially in NLOS settings, the link must be able to quickly adapt to changes in the transmitter or receiver locations if one or both of them are mobile. In practice, we would not expect these small-scale fluctuations to exhibit the degree of regularity seen here, due to the presence of surface irregularities, more complex scattering environments, and multipath reflections that are not purely specular.

4.2 Performance with Beamsteering/MMSE

Fig. 6 plots the spectral efficiency for the beamsteering/MMSE scheme, averaged over randomized transmitter coordinates, as a function of the per-antenna transmit power. When the LOS is unobstructed, the spectral efficiency approaches the $4N$ bps/Hz constellation-constrained limit at approximately $P_A = -5$ dBm. As before, LOS blockage significantly decreases the received SNR and capacity. Roughly 10 dBm of additional power is required to offset the performance degradation caused by LOS blockage.

The spectral efficiency is plotted as a function of transmitter position in Fig. 7 with $N = 2$ and $P = -10$ dBm. The sum-rate capacity approaches the 8 bps/Hz limit when the transmitter is placed near the center of the room. Uncoded data can be transmitted at a symbol error rate of $P_e \leq 10^{-5}$ through 85.5% of the room and a symbol error rate of $P_e \leq 10^{-10}$ through 73.5% of the room. When the channel is ill-conditioned, such as when the transmitter is placed in one of the front corners, an adaptive link can maintain a low error rate by increasing the transmit power, reducing the constellation size (e.g. QPSK or BPSK), or coding the data symbols. Rotating the transmitter to face the receiver, rather than the front wall, reduces spatial correlation at these locations.

Through 86% of the room, the transmitter beamsteers both signals in the direction of the LOS path. If the LOS channel component is ill-conditioned, which occurs in the front corners of the room, the spectral efficiency is increased by beamsteering one or both subarrays along a reflected path.

The spectral efficiency in the NLOS scenario is shown in Fig. 8. It is approximately 2 bps/Hz lower than with

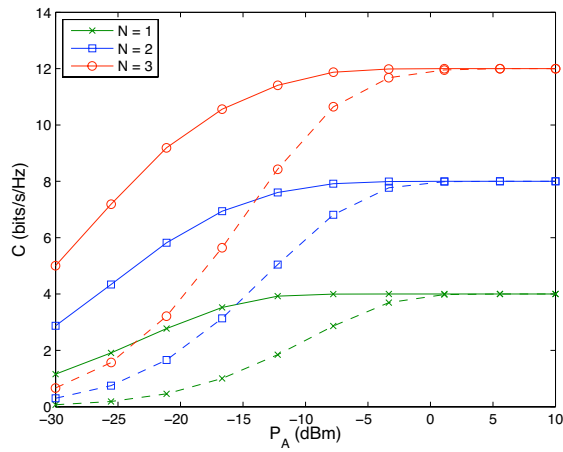


Figure 6: Spectral efficiency for the beamsteering/MMSE scheme as a function of P_A . Dashed lines represent the NLOS scenario.

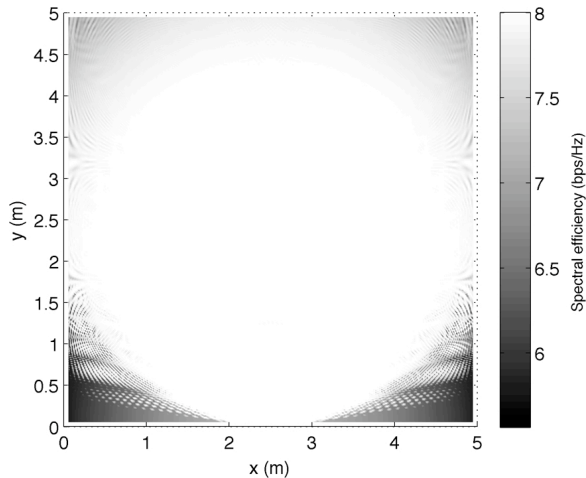


Figure 7: Spectral efficiency of beamsteering/MMSE scheme as a function of transmitter coordinates.

eigenmode transmission, and never approaches the 8 bps/Hz limit. Reliable uncoded transmission at this rate requires an additional 15 - 20 dBm of power. Alternatively, the transmitter can introduce coding or choose a smaller constellation. When the transmitter is placed near the left or right wall, steering both beams towards the reflected path off of that wall is optimal. Otherwise, the beamsteering subarrays typically beamsteer in different directions to maximize capacity.

5. CONCLUSIONS

The array of subarrays transceiver architecture presented here provides both directivity gain and spatial multiplexing gain. The directivity gain implies that the transmit power per transmit element can be reduced to levels that are easily achieved by CMOS power amplifiers, and that the channel seen by each data stream has minimal dispersion (more study is needed as to whether temporal equalization can be completely dispensed with). The spatial multiplexing gain

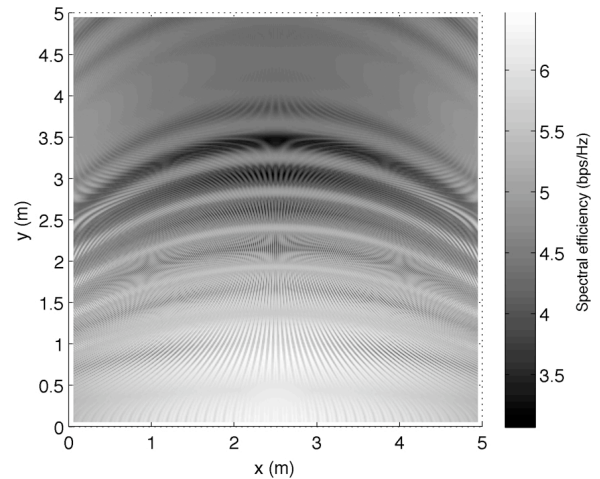


Figure 8: Spectral efficiency of beamsteering/MMSE scheme assuming LOS blockage.

is found to be robust to LOS blockage, although adaptive coding and modulation may be required to handle the lower SNR in these settings. The capacity benchmark provided by eigenmode transmission fluctuates significantly with the location of the transmitter and receiver within the room, but fixing the constellation size reduces these fluctuations by capping the achievable throughput.

6. REFERENCES

- [1] A. Arvanitis, G. Anagnostou, N. Moraitis, and P. Constantinou. Capacity study of a multiple element antenna configuration in an indoor wireless channel at 60 GHz. In *Vehicular Tech. Conf., IEEE 65th*, pages 609–613, April 2007.
- [2] D. Gesbert, H. Bolcskei, D. Gore, and A. Paulraj. Outdoor MIMO wireless channels: models and performance prediction. *IEEE Trans. Commun.*, 50(12):1926–1934, Dec. 2002.
- [3] T. S. Rappaport. *Wireless Communications: Principles and Practice*. Prentice Hall, New Jersey, 2002.
- [4] I. Sarris and A. Nix. Design and performance assessment of maximum capacity MIMO architectures in line-of-sight. *Communications, IEE Proc.*, 153(4):482–488, August 2006.
- [5] K. Sato, H. Kozima, H. Masuzawa, T. Manabe, T. Ihara, Y. Kasashima, and K. Yamaki. Measurements of reflection characteristics and refractive indices of interior construction materials in millimeter-wave bands. In *Vehicular Tech. Conf., IEEE 45th*, volume 1, pages 449–453, 25-28 1995.
- [6] C. Sheldon, M. Seo, E. Torkildson, M. Rodwell, and U. Madhoo. A 2.4 Gb/s millimeter-wave link using adaptive spatial multiplexing. *IEEE Int. AP-S Symp.*, July 2010.
- [7] P. F. M. Smulders. Deterministic modelling of indoor radio propagation at 40-60 GHz. *Wireless Personal Communications*, 4(2):127–135, June 1994.
- [8] H. Xu, V. Kukshya, and T. Rappaport. Spatial and temporal characteristics of 60-GHz indoor channels. *IEEE J. Sel. Areas Commun.*, 20(3):620–630, April 2002.